Lawrence Berkeley Laboratory
UNIVERSITY OF CALIFORNIA

Submitted to Physics Letters B

ONE- AND TWO-PROTON INCLUSIVE SPECTRA IN 800 MeV PROTON-NUCLEUS COLLISIONS AND THE MEAN FREE PATH OF PROTONS IN NUCLEI

I. Tanihata, S. Nagamiya, S. Schnetzer, and H. Steiner

October 1980

Prepared for the U.S. Department of Energy under Contract W-7405-ENG-48

DISCLAIMER

One- and Two-Proton Inclusive Spectra in 800 MeV Proton-Nucleus Collisions and the Mean Free Path of Protons in Nuclei

I. Tanihata,[a] S. Nagamiya, S. Schnetzer, and H. Steiner

Lawrence Berkeley Laboratory and Department of Physics,
University of California, Berkeley, CA 94720

One- and two-proton inclusive spectra have been measured in collisions of 800 MeV protons with C, NaF, KCl, Cu, and Pb targets. The single proton inclusive yield increases monotonically with target mass, while the two-proton yield at $\theta_{Lab} = \pm 40^{o}$ associated with pp quasi-elastic scatterings shows a maximum at a mass number of about 50. A model calculation reproduces the observed target mass dependence with a mean free path of $\sim$2.5 fm for 800 MeV protons inside the nucleus.

The mean free path, λ, of nucleons inside the nucleus is one of the fundamental quantities in the study of pA (proton-nucleus) and AA (nucleus-nucleus) collisions. If λ is much smaller than the typical reaction size, R, processes involving multiple NN (nucleon-nucleon) collisions play a dominant role. It is in this case that thermal models [1], hydrodynamical models [2], or other statistical models may have their greatest chance of success. On the other hand, if $\lambda >> R$, processes involving single NN collisions become dominant, and models such as those suggested by Blankenbecler and Schmidt [3], or by Hatch and Koonin [4] tend to be more appropriate. Therefore, by determining the value of λ and R experimentally we expect to gain a clearer understanding of the reaction dynamics. Recent measurements of two-pion correlations [5], composite particle productions [6] and pion inclusive spectra [7] have suggested that the reaction size in AA collisions at $\sim$1 GeV/nucleon is 3-4 fm. In this paper we report the measurement of the single proton inclusive ($p + A \rightarrow p + X$) and the two proton coincidence ($P + A \rightarrow 2p + X$) spectra. The proton mean free path inside the nucleus is then estimated from the target-mass (A) dependence of the two-proton coincidence yield which is associated with pp quasi-elastic-scattering (QES).

A proton beam of 800 MeV from the Berkeley Bevatron was incident on C, NaF, KCl, Cu, and Pb targets. The magnetic spectrometer described in Ref. [8] was used to detect protons at laboratory angles (θ) from 15^{o} to 60^{o} and for momenta between 0.5 and 2.0 GeV/c. When the spectrometer was set at $\theta = 40^{o}$, two-proton coincidences were measured as well. For this purpose three counter telescopes, which were the same as those described in Refs. [8] and [9], were used. These telescopes, named the R ,U ,and D telescopes, were located at scattering angles of $(\theta,\phi) = (40^{o}, 180^{o})$ and $(40^{o}, 90^{o})$, respectively, and the coincidence count between one of these and the spectrometer was measured.

Since the spectrometer was located at $\phi = 0^{\circ}$, its coincidence with the R-telescope indicates that the two protons are emitted in the same reaction plane. Each telescope consisted of three plastic scintillators with absorbers sandwiched in between. A triple coincidence between these scintillators corresponds to proton energy of more than 200 MeV.

Fig. 1(a) shows inclusive single-proton momentum spectra for the C target. At small angles (15° and 30°) the spectra show strong peaks due to pp or pn QES, while at large angles they are much smoother. Fig. 1(b) shows the spectra at 40° in more detail. Shown there are the single-proton spectrum (solid circles), the proton spectrum in coincidence with the in-plane (R) telescope (open circles), and the proton spectrum in coincidence with the out-of-plane (U or D) telescope (squares). A sharp peak is observed in the coincidence spectrum with the in-plane telescope. The momentum of this peak position agrees well with the expected proton momentum due to pp QES in which two protons are emitted at $(\theta,\phi) = (40^{\circ}, 0^{\circ})$ and $(40^{\circ}, 180^{\circ})$. On the other hand, a structureless spectrum is observed when the coincidence with the out-of-plane telescope is taken. Curve A in the figure shows the result of the plane-wave-impulse approximation for the one-proton spectrum [10]. It deviates substantially from the data, particularly at high momentum. Curve B shows the result of a linear cascade calculation by Knoll and Randrup [11], which includes effects due to multiple scatterings within each linear tube. The shape of the spectrum is reproduced much better by this calculation. Curves C and D show the linear cascade results [11] for the in-plane and the out-of-plane coincidence, respectively. Agreement with the out-of plane coincidence is good, but the in-plane coincidence prediction is a factor of $\sim$2.5 larger than the data. Since this calculation includes only cascades in a straight line geometry, it may underestimate the rescattering effects.

Fig. 2(a) shows the A-dependence of the QES cross sections at 15^{o}, which are obtained by integrating the single-proton spectra near the QES peak. The cross section monotonically increases roughly in proportion to $A^{1/3}$, which is characteristic of protons produced in surface reactions. The integrated cross sections agree with a recent result by Chrien et al. [13], although the present QES spectrum at 15^{o} is broader than theirs because of the wide angular acceptance of our spectrometer ($\pm 3^{o}$). On the other hand, the single-proton cross section at low momentum as well as the out-of-plane coincidence yield show a stronger A-dependence ($\sim A^{2/3}$), suggesting contributions from multiple scatterings.

Fig. 2(b) shows the A-dependence of QES cross sections obtained from the coincidence measurement. To evaluate the QES cross section for each target, a gaussian fit was made to the QES peak after subtracting the out-of-plane coincidence spectrum from the in-plane coincidence spectrum, as shown in Fig. 3. The widths (σ) of the fitted Gaussians [$\exp(-(p-p_0)^2/\sigma^2)$] are almost independent of target and are $\sim$160 MeV/c. The two-proton QES cross section has a maximum at around A = 50 and then decreases as the target mass increases further. This A-dependence is strikingly different from that of the single-proton cross sections which increase monotonically with A. As the target mass increases, the probability of NN scattering increases, but at the same time the probability of rescatterings after the first collision increases as well. The reduction of the QES cross sections due to rescattering is larger when two protons are detected than for a single proton because events are lost if either one of the nucleons is rescattered.

We parameterize the rescattering process by the mean free path of protons inside the nucleus. Under the assumption that the target nucleus has a

uniform nucleon density (ρ) within a radius (r) given by $r = (1.28\ A^{1/3} - 0.76 + 0.8\ A^{-1/3})$ fm [12], the single-proton QES cross section is given by

$$\frac{d\sigma}{d\Omega_1} = \frac{1}{A}\left(Z\frac{d\sigma_{pp}^{el}}{d\Omega_1} + N\frac{d\sigma_{pn}^{el}}{d\Omega_1}\right)\int \rho\, dV \exp\left(-\frac{\ell^{in}}{\lambda^{in}}\right)\exp\left(-\frac{\ell_1^{out}}{\lambda_1^{out}}\right), \qquad (1)$$

where A, Z, and N are the mass, the proton, and the neutron numbers of the target nucleus, respectively, and $d\sigma_{pp}^{el}/d\Omega_1$ ($d\sigma_{pn}^{el}/d\Omega_1$) is the differential cross section of pp (pn) elastic scattering. The attenuations of incident and out-going protons are parameterized by energy dependent mean-free paths λ^{in} and λ^{out}. The path lengths of protons from the nuclear surface to the interaction point are labeled by ℓ^{in} and ℓ^{out}. Integration is made for the whole target volume.

For the two-proton QES cross section, an additional attenuation factor for the second proton is included. In addition, $d\sigma^{el}/d\Omega_1$ becomes a double differential cross section $Z(d^2\sigma_{pp}/d\Omega_1 d\Omega_2)$; thus

$$\frac{d^2\sigma}{d\Omega_1 d\Omega_2} = \frac{Z}{A}\frac{d^2\sigma_{pp}^{el}}{d\Omega_1 d\Omega_2}\int \rho dV \cdot \exp\left(-\frac{\ell^{in}}{\lambda^{in}}\right)\cdot\exp\left(-\frac{\ell_1^{out}}{\lambda_1^{out}}\right)\cdot\exp\left(-\frac{\ell_2^{out}}{\lambda_2^{out}}\right). \qquad (2)$$

In Eqs. (1) and (2) three values of the mean free paths, λ^{in}, λ_1^{out}, and λ_2^{out} appear. They generally depend on the proton energy, E_p, and the Z/N ratio of the target nucleus. We assume that such dependences are parameterized by

$$\lambda \propto A / (Z\sigma_{pp}(E_p) + N\sigma_{pn}(E_p)), \qquad (3)$$

where $\sigma_{pp}(E_p)$ and $\sigma_{pn}(E_p)$ are free pp and pn total cross sections, respectively. We thus have one parameter left which we take to be

$$\lambda \equiv \lambda^{in} \text{ (for } Z=N), \qquad (4)$$

which is the mean free path of an 800 MeV proton inside the Z = N target.

In Fig. 2(b) the calculated A-dependences are shown for several values of λ, where absolute scales are arbitrarily adjusted. A mean free path of 2.5 fm gives the best fit to the data. In the single-proton data, an absolute comparison between Eq. (1) and the data can be made after integration of the cross section over the QES peak. Such an integration can most unambiguously be done at 15^{o} because of the dominance of QES. Comparison between the data and the calculated values (solid curve) is shown in Fig. 2(a). Although the calculated values are systematically smaller than the data the agreement is fair.

The observed mean free path λ (at 800 MeV) = 2.5 fm is longer than the value expected from free nucleon cross sections (λ_{free} = 1.6 fm). The present calculations are based on several assumptions and simplifications. First, we neglected the effect of Fermi motion in the calculations. Because we used for comparison the data integrated over the QES peak, we believe that this is not an important effect. Secondly, we assumed that any protons which are scattered before or after the QES of interest are not detected. This assumption could be too strong, since any small angle scattering without significant momentum change would still be detected as a QES scattering. The observed longer mean free path compared to λ_{free} may be due, at least in part, to this assumption. Thirdly, we assumed that the target nucleus is a sharp sphere. The actual nucleus has a diffuse surface where the nucleon density is small. We have extended our calculations to a folded Yukawa-type density distribution [12] using free NN cross sections. For the two-proton data the calculated results show almost constant yields over a wide range of target masses with a slight peak at around A = 50. The fits, however, are considerably worse than the best fit obtained from the sharp-sphere assumption. This suggests,that

the effective NN cross section may be larger at the nuclear surface than inside, an effect qualitatively consistent with expectations based on Pauli exclusion principle suppresion. Finally, it is worth noting that the mean-free-path evaluated from an optical potential analysis [13], $\lambda = 3.6$ fm, is longer than the value obtained here.

In conclusion, we have observed strong peaks in the inclusive data due to NN QES at small angles, but at large angles the QES peak appears only when the second particle is detected in the same reaction plane. The study of the A dependence of inclusive and two-proton coincidence yields, especially the latter, shows that such measurement can be used to determine the mean fee path of nucleons inside the nucleus. Within the framework of the simple analysis described above we estimate that the mean free path is about 1.6 times longer than the value expected from free NN collisions. To understand these results further studies of small angle scattering, as well as the reduction of the NN cross section due to the Pauli effect, are necessary. Finally, the value of λ turned out to be comparable to R where R is the reaction size of AA collisions. This fact implies that both the single and multiple NN collisions are highly intermingled in AA collisions.

The authors would like to thank O. Chamberlain, M.-C. Lemaire and G. Shapiro for their help throughout this work. We are also grateful to J. Knoll, J. Randrup and W. Myers for fruitful discussions. This work was supported by the Nuclear Science Division of the U.S. Department of Energy, the INS-LBL Collaboration Program, and a grant from the Commemorative Association for the Japan World Exposition. This work was partially supported by the U.S. Department of Energy under Contract W-7405-ENG-48.

REFERENCES

a) On leave from INS, University of Tokyo, Tanashi, Tokyo, Japan.

[1] G. D. Westfall et al., Phys. Rev. Lett. 37 (1976) 1202.

[2] A. A. Amsden, F. H. Harlow and J. R. Nix, Phys. Rev. C15 (1977) 205.

[3] I. A Schmidt and R. Blankenbecler, Phys. Rev. D15 (1977) 3321.

[4] R. L. Hatch and S. E. Koonin, Phys. Lett. 81B (1978) 1.

[5] S. Y. Fung et al., Phys. Rev. Lett. 41 (1978) 1592.

[6] M.-C. Lemaire et al., Phys. Lett 85B (1979) 38.

[7] Meng Ta-Chung, Phys. Rev. Lett. 42 (1979) 1331.

[8] S. Nagamiya et al., J. Phys. Soc. Japan, supplement 44 (1978) 378; Phys. Lett. 81B (1979) 147.

[9] I. Tanihata, M.-C. Lemaire, S. Nagamiya, and S. Schnetzer, Phys. Lett. (in press), LBL-10694 (preprint).

[10] Y. Alexander et al., Phys. Rev. Lett. 44 (1980) 1579.

[11] J. Knoll and J. Randrup, LBL-11418 (to be published).

[12] W. D. Myers and W. J. Swiatecki, LBL-9306 and private communication.

[13] R. E. Chrien et al., Phys. Rev. C21 (1980) 1014.

FIGURE CAPTIONS

Fig. 1. Single-proton inclusive spectra (a) and the coincidence spectra at $\theta_1 = \theta_2 = 40^\circ$ (b) for 0.8 GeV p + C reactions. Solid curves in (a) are drawn for guiding the eye. Arrows indicate the proton momenta from pp or pn QES. Curves in (b) show the results of theoretical calculations. See the text for details.

Fig. 2 Target-mass dependence of the single-proton QES cross section (a) and the two-proton QES cross section (b). Curves in the figure show the result of the calculations based on Eqs. (1) and (2) with the mean free path λ of the 0.8 GeV protons as a parameter. Best fit is obtained for $\lambda = 2.5$ fm.

Fig. 3. Proton spectra at $\theta = 40^\circ$ obtained by subtracting the out-of-plane coincidence spectra from the in-plane coincidence spectra. Dotted curves indicate the gaussian fit to the data. Scale of cross sections is arbitrary except for relative scales for different targets.

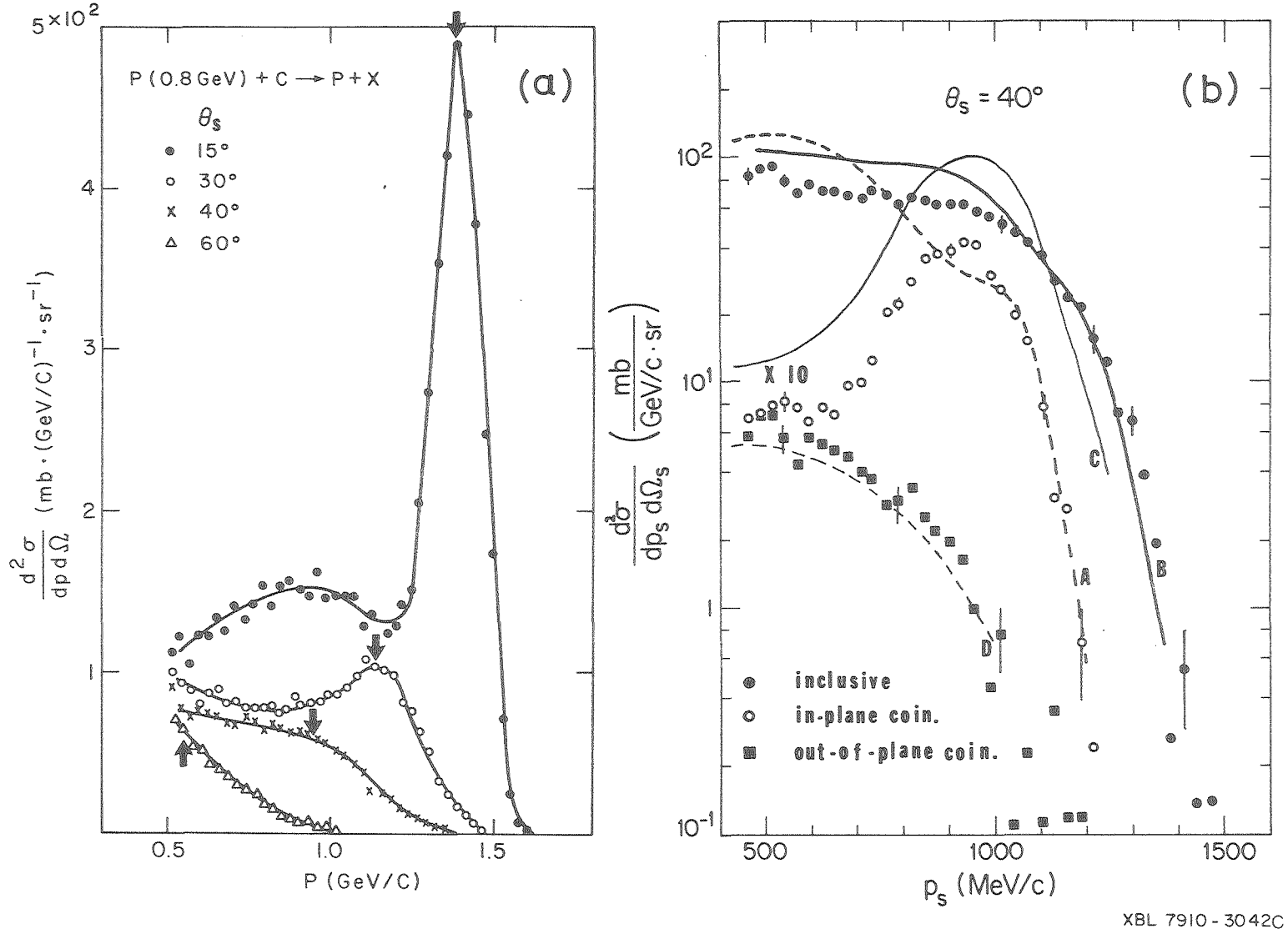
P (0.8 GeV) + C → P + X
(a)
θs
15°
30°
40°
60°
5×10²
4
3
2
1
0.5
1.0
1.5
P (GeV/C)
d²σ/dp dΩ (mb·(GeV/C)⁻¹·sr⁻¹)
θs = 40°
(b)
10²
10¹
1
10⁻¹
X 10
A
B
C
D
inclusive
in-plane coin.
out-of-plane coin.
500
1000
1500
ps (MeV/c)
d²σ/dps dΩs (mb/GeV/c·sr)
XBL 7910-3042C

Fig. 1

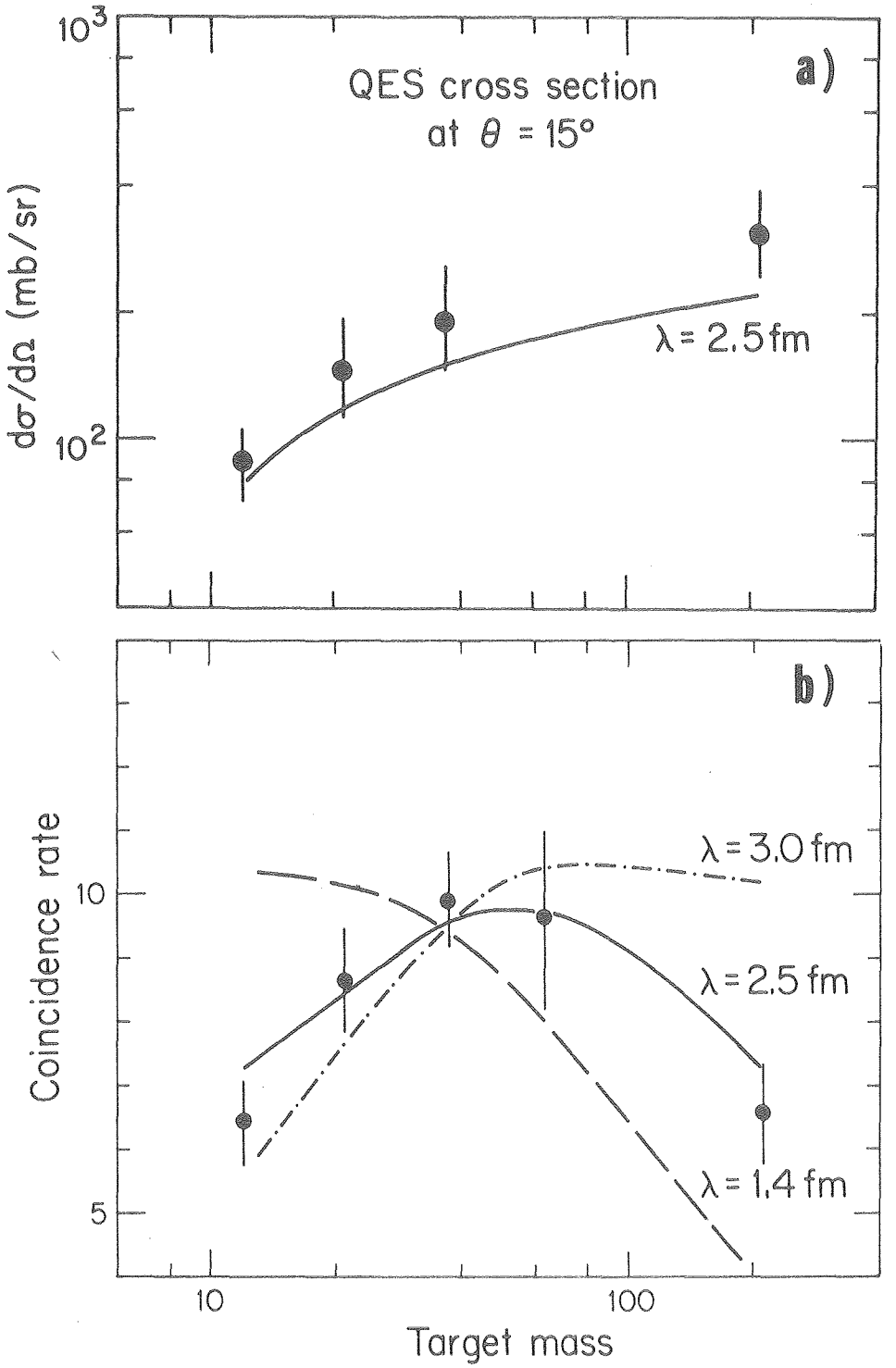
a)
QES cross section
at θ = 15°
dσ/dΩ (mb/sr)
10³
10²
λ = 2.5 fm
b)
Coincidence rate
10
5
λ = 3.0 fm
λ = 2.5 fm
λ = 1.4 fm
10
100
Target mass
XBL 7910-3040A

Fig. 2

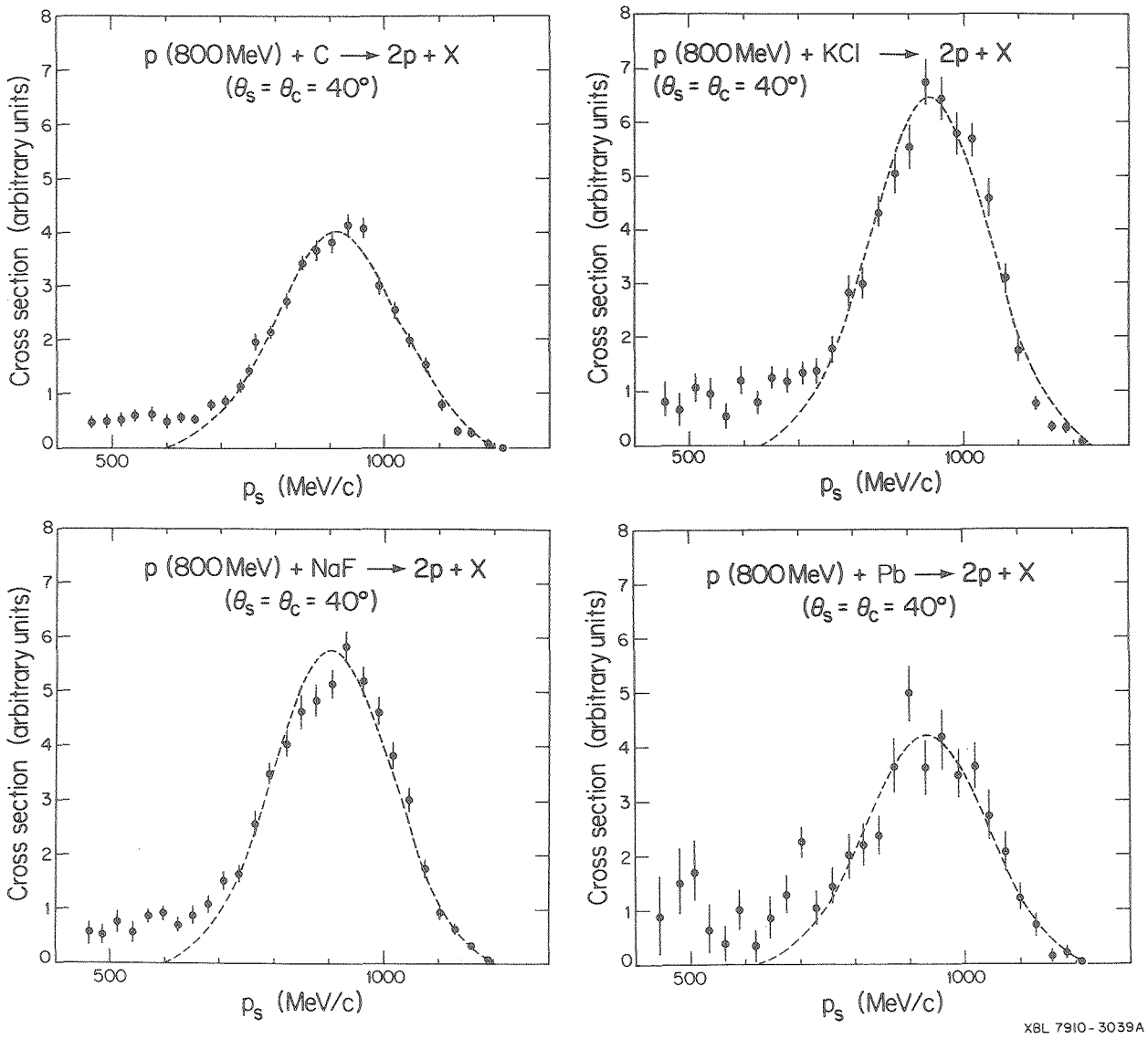
p (800 MeV) + C → 2p + X
(θs = θc = 40°)
p (800 MeV) + KCl → 2p + X
(θs = θc = 40°)
p (800 MeV) + NaF → 2p + X
(θs = θc = 40°)
p (800 MeV) + Pb → 2p + X
(θs = θc = 40°)
Cross section (arbitrary units)
ps (MeV/c)
500
1000
0
1
2
3
4
5
6
7
8
XBL 7910-3039A